

Investigation on Luminescence near Focal Point during Ultrafast Laser Microwelding of Glass Substrates

Junpei Fujiwara^{*1}, Hikari Okuno², Taiga Sasahara², Takao Ota^{1,2}, Wataru Watanabe³, and Takayuki Tamaki^{*1,2}

¹ Advanced Mechanical Engineering Course, Faculty of Advanced Engineering Control Engineering, National Institute of Technology (KOSEN), Nara College, 22 Yata-cho, Yamatokoriyama, Nara 639-1080, JAPAN

² Department of Control Engineering, National Institute of Technology (KOSEN), Nara College, 22 Yata-cho, Yamatokoriyama, Nara 639-1080, JAPAN

³ Department of Electrical & Electronic Engineering, College of Science and Engineering, Ritsumeikan University, 1-1-1 Nojihigashi, Kusatsu, Shiga, 525-8577 Japan

*Corresponding author's e-mail: jfujiwara@class.ctrl.nara-k.ac.jp, tamaki@ctrl.nara-k.ac.jp

In this study, we investigate luminescence near focal point during ultrafast laser microwelding in order to find the optimal processing position for sealing of two glass substrates. To quantitatively analyze the emission near the focal point during ultrafast laser microwelding, the focal position was shifted vertically by 0.01 mm increments from the boundary surface of the glass substrates. In addition, we extracted video frames at intervals of 0.1 seconds during processing and displayed the emission images near the focal point by decomposing them into the color components of RGB. As a result, the welding status can be determined based on the temporal changes in luminescence at each focal point position. Furthermore, it was found that the changes in the RGB components were largely influenced by the air between the glass substrates.

DOI: 10.2961/jlmn.2024.02.2009

Keywords: ultrafast laser microwelding, femtosecond laser, glass, microwelding, luminescence

1. Introduction

These days, various industrial products are becoming smaller, more functional, and denser. Laser welding is used as a means of bonding materials with high precision and microscopic accuracy because laser light is highly focused, making it suitable for high-precision, localized welding [1-3]. In semiconductors and electronic components, which are indispensable to industry, lasers are also used as a sealing technology to prevent component deterioration and to improve insulation. Particularly, organic materials such as OLED (organic LED) displays are unsuitable for sealing using sintering furnaces because organic materials are sensitive to heat and moisture, making laser welding, which has a small range of thermal effects, useful.

For laser welding (sealing) of transparent materials such as glass, a light-absorbing material (intermediate layer) must be placed between the materials to be welded. For this reason, resin or frit glass is used as a sealant between the glass substrate and the cover glass. However, the use of an interlayer requires the cost of the sealant and the time and effort necessary to place it. It also causes misalignment in the interlayer, making fine welding difficult.

Ultrafast laser microwelding is used to resolve these difficulties. Ultrafast laser pulses are characterized by their extremely short pulse widths of less than picoseconds and the resulting high peak power. The high peak power of ultrafast laser pulses causes nonlinear absorption phenomena near the focal point (Fig. 1). Nonlinear absorption phenomena include avalanche ionization, in which a generated free electron is accelerated by the energy of a subsequent light pulse and collides with other electrons to generate free electrons, and multiphoton absorption, in which multi-

ple photons are simultaneously absorbed to enable processing of transparent materials even with pulsed light having energy below the band gap energy. The resulting plasma, heat, and shock waves can locally melt the glass material. Therefore, glass materials can be welded together directly without an intermediate layer, which is easier and finer welding than welding using an intermediate layer [4-7]. Also, the velocity of electrons travelling in the lattice can reach 100 000 m/s. This high velocity allows the electrons to penetrate deeper into the lattice without energy transfers to the lattice. In addition, the heat-affected zone is very small, as there is no heat conduction during pulse irradiation and lattice heating. Therefore, faster and more precise machining is possible because of the higher beam quality and lower thermal effects [8].

When using ultrafast laser microwelding to weld large areas, it is important to adjust the focal point. This is because the focal point determines whether the welding is possible or not, as well as the strength of the welding. However, the gap width and distortion between samples vary depending on the sample type and fixation method. Therefore, a program that automatically adjusts the optimum position would be useful [9,10]. The plasma emission of lasers has been found to be suitable for monitoring the welding process by Hecker et al [9,10]. On the other hand, it does not accurately detect cracks, which are an important factor in joint quality. In addition, depending on the component and material used, light from the side (internal light) may not be available.

In this study, we develop an evaluation method that can search for optimal processing conditions by utilizing the changes in the color and intensity of the light generated

during laser irradiation over time, depending on the position of the laser beam focus on the material. We analyze the light generated during laser irradiation through image analysis, quantitatively determining the changes in emission at the focal point and derive the optimal processing conditions based on the analysis results.

2. Experimental method

2.1 Experiment equipment and materials

The optical setup used for this experiment is presented in Fig. 2. For the microwelding, we used a burst-mode femtosecond laser system (Light Conversion, UAB, PHAROS, PH2-1mJ-SP), which generates 1030 nm, 190 fs, and 1 MHz ultrafast laser pulses with a pulse energy of 1.5 μ J. The sample to be welded was white glass substrate (Schott, B270, 50 mm \times 50 mm \times 1 mm thickness). The laser beam output from a femtosecond laser source was reflected by a mirror and focused on glass substrates through a half-wave plate, a polarizer, and an objective lens ($\times 20$, NA 0.40). After a power meter (PM120 and S310A; ThorLabs Inc.) was placed between the shutter and the dichroic mirror, the output power was adjusted using the half-wave plate. Polarizer is used to adjust the light to circular polarization. A beam damper and shutter were placed along the path to shield the laser beam temporarily. The dichroic mirror allowed observation of processes using a CCD camera.

2.2 Experimental method

First, the welding conditions in this experiment are described. The two glass substrates were stacked, and applied pressure for eliminating the airgap between two glass substrates with a fixture on a two-dimensional translation stage (Fig. 3). The pressure was checked by Arduino Uno using a sensor and adjusted to be even. The sample was translated 10 mm long with a scan speed of 1 mm/s. In this experimental setup, the relationship between output power and scanning speed is known. In this experiment, an output of 1.5 μ J and a scanning speed of 1 mm/s, which are considered optimal, are used. In addition, as the scanning speed changes, the heat-affected amount at the processing area changes. Therefore, if the scanning speed is small compared to the output, cracks and ablation will occur, and if the scanning speed is large, sufficient joint strength will not be ensured. To quantitatively analyze the emission near the focal point during ultrafast laser micro-welding, the focal position was shifted vertically by 0.01 mm increments from the boundary surface of the glass substrates (Fig. 4). In this experiment, "+" refers to moving downward from the boundary surface, while "-" refers to moving upward from the boundary surface. The moving images during processing were then acquired by a CCD camera. Using OpenCV-python, the video was cut into discrete images at every 0.1 second frame. The cropped image was again decomposed into its RGB components using OpenCV-python, and the obtained results were graphed, and the obtained data were analyzed (Fig. 5). During welding, molten glass flows into the space between the glass substrates. This may cause a change in the light generated by the plasma. It is also thought that the light changes differently when the light is focused between the samples and when the light is focused inside the samples. When light is re-

fracted by glass distortion, the refractive index varies with wavelength. Therefore, in this experiment, light is separated into its RGB components and analyzed in detail. If the welding is uniform, the temporal variation of the light is considered to be small.

3. Experiment result

3.1 RGB components

Figure 6 shows the temporal change of RGB components at focal positions of -0.04 mm (Fig. 6 (a)) and +0.05 mm (Fig. 6 (b)). (a) is processing within the weldable range and (b) is processing out of the weldable range. In the graph, the time at which the maximum value is reached represents the start time of the processing, and the time at which the value becomes "0" represents the end time of the processing. It can be observed that in (a), the temporal variation of each element is smaller compared to (b). In addition, certain values are detected before and after processing, indicating that external factors may be influencing the values. However, since the values immediately after processing become "0", it is necessary to investigate whether they actually have an influence during processing. The temporal variation of each value is caused by the plasma at the welding area, refraction of light by the molten glass, and changes in the processing surface. Of these factors, the first two are considered to vary little unless there is a large change in the focal point, because the laser's focusing diameter is constant. The large change in focus position here does not depend on whether or not welding is possible. On the other hand, the processing surface is considered to have a significant effect. Changes in the processing surface include cracks and voids. Figure 6 shows images of the processing surface at 7.3 seconds at the -0.04 mm and +0.05 mm focal points. At the +0.05 mm focal point, a crack can be seen to the left of the processing area, as shown in the figure. Figure 5 also shows that a large change in the RGB component occurred at that time. Since the welding strength decreases when there are many cracks and voids, the focal point with a large change in the RGB component is not considered to be the optimal processing position. Therefore, it may be possible to determine the quality of the welding from the RGB components.

3.2 The standard deviation of the RGB components

Figure 8 also shows the standard deviation of the RGB components at each focal point. (a) shows the standard deviation for all RGB components, while (b) shows the standard deviation for the blue component only. The standard deviation represents the amount of change in each element over time. The large value means that the light changes significantly during processing, which may indicate that stable welding has not been achieved. In addition, Figure 10 shows the width of the processing trace at each focal point position within the welding range. The width of the processing trace in this context refers to the width of the heat-affected zone during the processing. The bonding area is the yellow area shown in the figure. In Figure 8, the yellow area is the focal point where the welding was successful. Figure 11 shows a CLSM image of the lower glass substrate at a focal point of -0.04 mm. As can be seen from Figure 8, Red, Green, and Blue have similar trends. On the other hand, unlike Blue, the values of Red and Green in-

crease in the central region. This appears to be related to the air between the glasses. As can be seen in Figure 9, no significant changes in values caused by cracks or other factors can be observed. The interglass widths vary slightly from place to place depending on distortion and pressure bias. This may have caused slight changes in the values.

Here, looking at Figure 10, it can be said that there is the highest correlation between the width of the processing trace and the values of the blue component. The reasons for the increase in the standard deviations for Red and Green need to be examined. Because the values could vary depending on the optical system and equipment, environmental and other disturbances should also be investigated. It

can also be seen that the extra heat-affected zone increases as the focal point moves away from the space between the glass specimens. Furthermore, Figure 11 shows the heat-affected zone outside of the bonding area. The area of high curvature is the bonding area, and its transparency is high in the image from above. On the others, cracks and other defects can be seen. From the above, it can be assumed that the time variation of the RGB component can represent the optimum processing position.

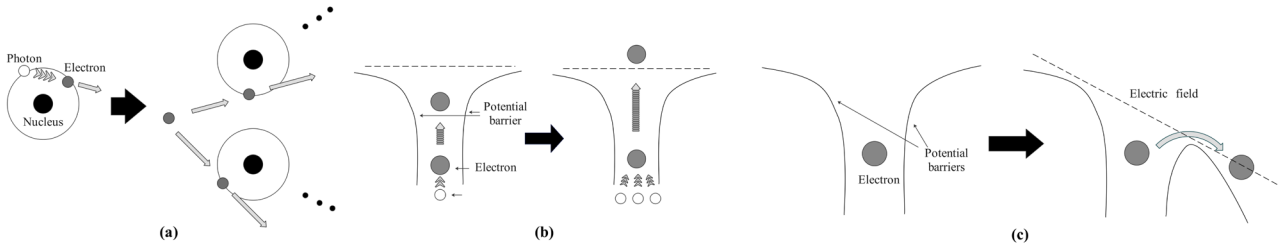


Fig. 1 Non-linear absorption phenomena
 (a) Avalanche ionization,
 (b) Multiphoton absorption phenomenon,
 (c) Tunnel ionization.

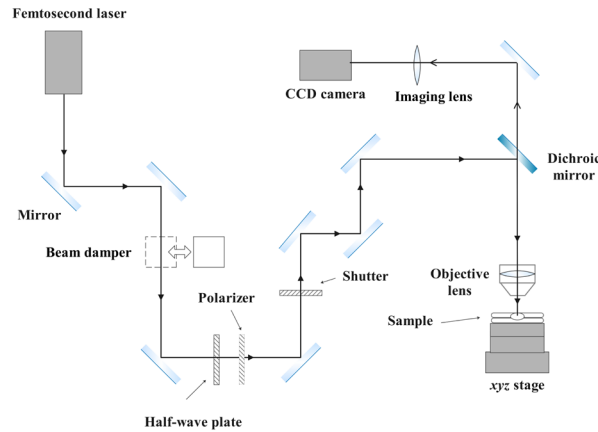


Fig. 2 Optical setup.

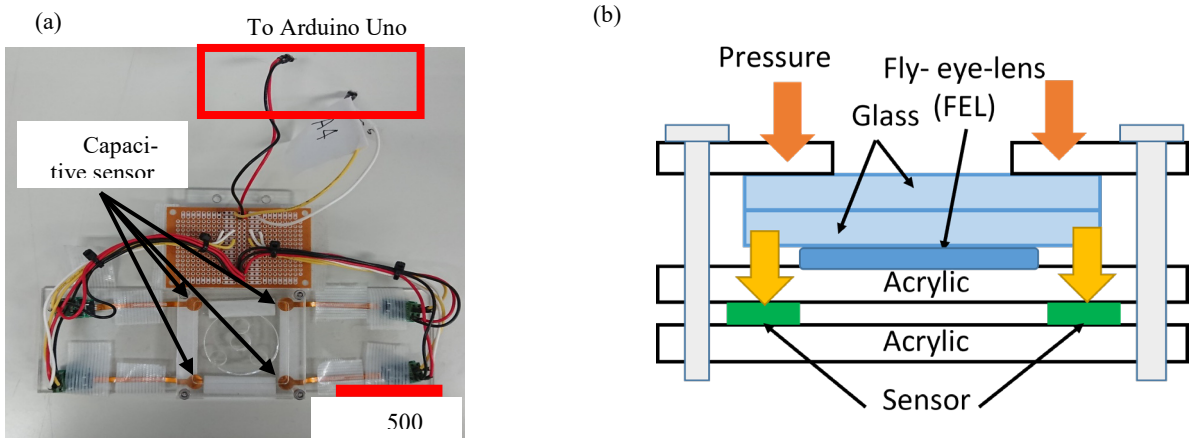


Fig. 3 Developed the fixture.
 (a) Top view, (b) Schematic diagram of cross-sectional view.

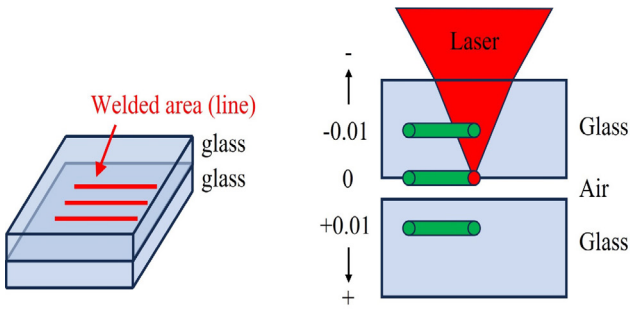


Fig. 4 Welding specifications.

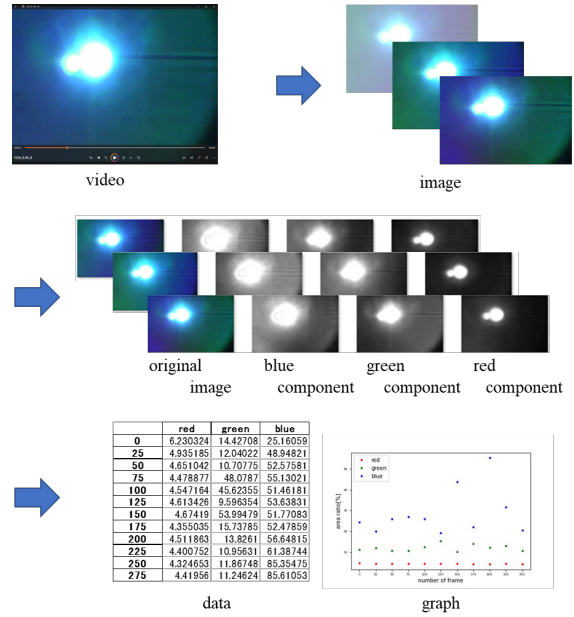
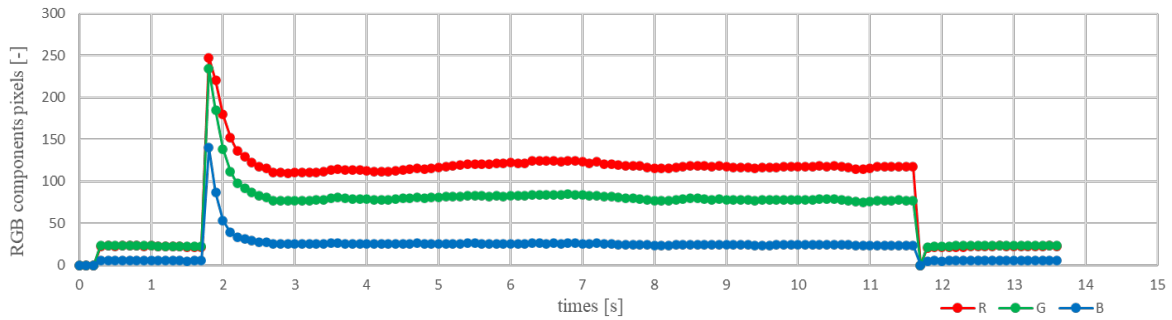
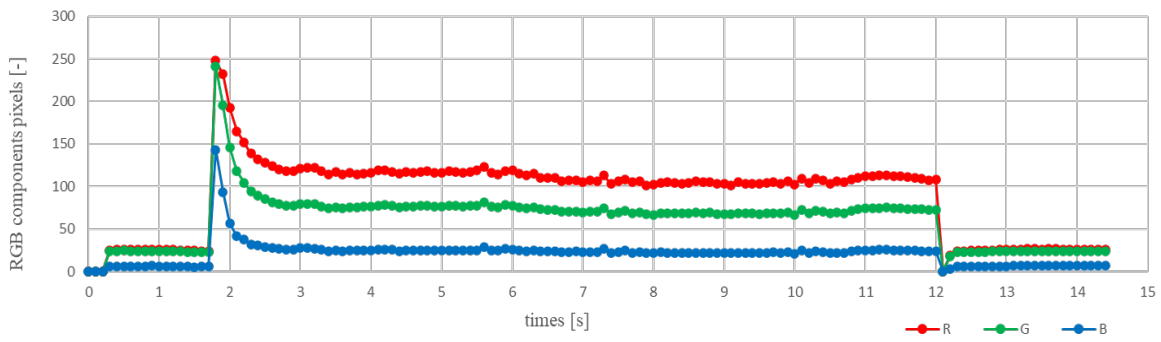


Fig. 5 Experimental method.



(a) Focal position of -0.04 mm



(b) Focal position of $+0.05$ mm

Fig. 6 Temporal change of RGB components.

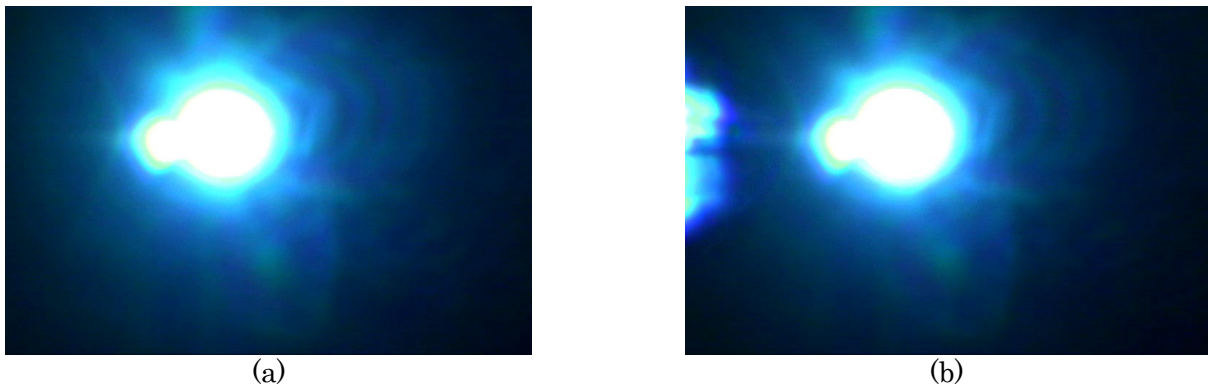
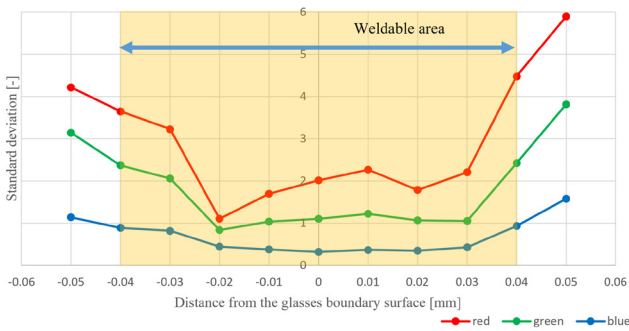
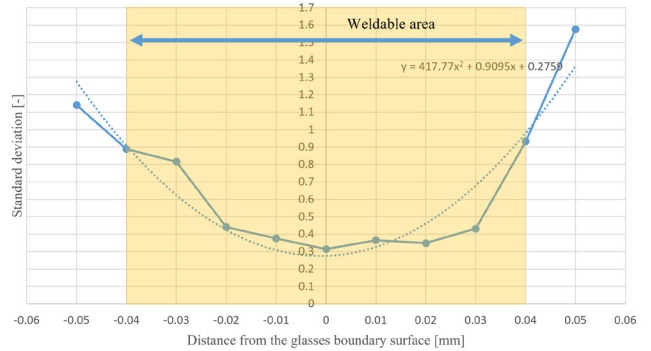


Fig. 7 Image of the processed surface at 7.3 seconds.
(a) Focal position of -0.04 mm, **(b)** Focal position of +0.05 mm.



(a) RGB components



(b) Blue

Fig. 8 The standard deviation of the RGB components at each focal point.

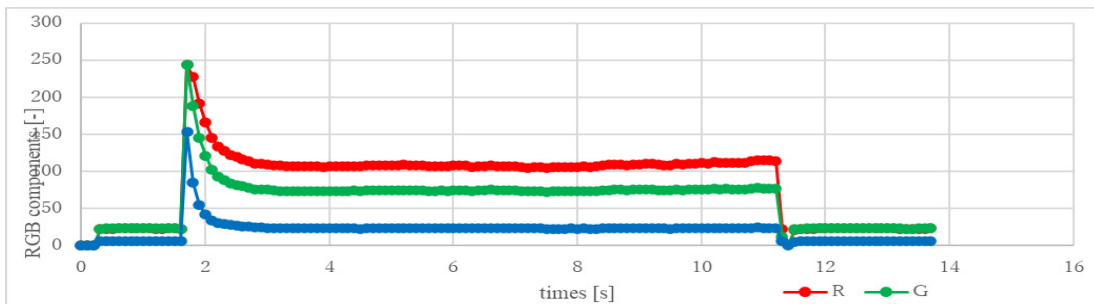


Fig. 9 Temporal change of RGB components at focal position of +0.01 mm.

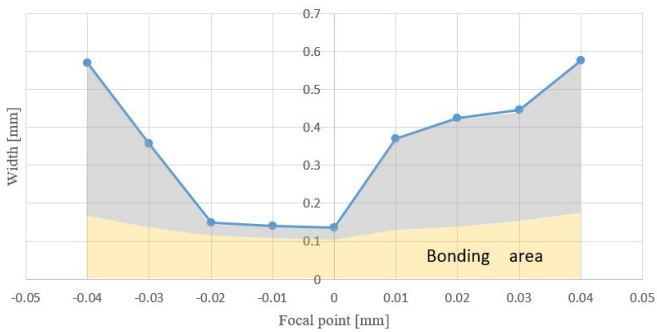


Fig. 10 Width the processing trace at each focal point.

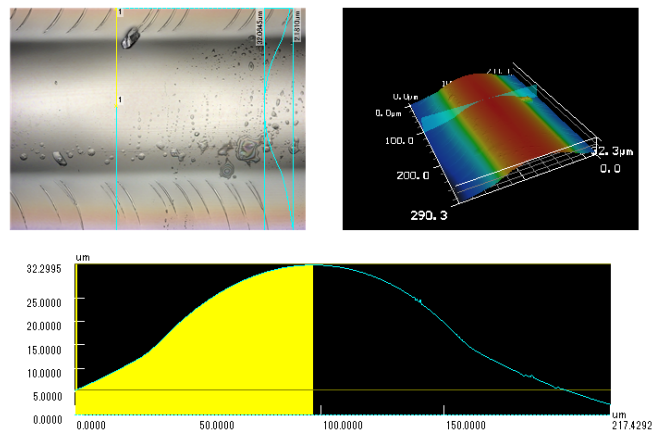


Fig. 11 CLSM image of the lower part of the processing trace at a focal point of -0.04 mm.

4. Conclusion

In this experiment, we investigated whether it would be possible to determine the bonding status by analyzing RGB-resolved images near the focal point when welding using the ultrafast microwelding. As a result, it was found that the Blue component might serve as a criterion for welding. Also, it has been discovered that the proportion of air to glass in the molten region may be an important factor causing the temporal change in each RGB component. Then, by measuring the distance between glass substrates, the relationship between the distance and the optimum focal point can be determined. On the other hand, if the distance between glass substrates cannot be fixed, it will result in a change in the optimal focal position. Currently, pressure is manually applied to the glass substrates using a pressure sensor, so a method that can measure the distance between glass samples will be needed in the future. One of these is the use of air pressure cylinders. This allows the pressure to be applied automatically and evenly to the entire area. It is also necessary to check for and eliminate errors due to environment or crisis. In addition, binding strength and other parameters should be measured to confirm that the results of this experiment are correct. This is because it is believed that the optimal welding conditions should be judged by the strength of the joint.

References

- [1] T. Arai, N. Asano, S. Suzuki, and H. Harada: *J. Jpn. Soc. Pre. Eng.*, 2013S (0), (2013) 579.
- [2] K. Atsumi: *Rev Laser Eng.*, 38, (2010) 60.
- [3] T. Tokunaga: *J. Jpn. Soc. Pre. Eng.*, 75, (2015) 595.
- [4] W. Watanabe and T. Tamaki: *J. Jpn. Soc. Pre. Eng.*, 81, (2015) 732.
- [5] T. Tamaki, W. Watanabe, and K. Itoh: *Opt. Express*, 14, (2006) 10460.
- [6] J. Fujiwara and T. Tamaki: *Appl. Phys. A*, 128, (2022) 1076.
- [7] H. Huang, L. Yang, and J. Liu: *Appl. Opt.*, 51, (2012) 2979.
- [8] S.-S. Wellershoff, J. Hohlfeld, J. Gdde, and E. Mathias: *Appl. Phys. A*, 69, (1999) 99.
- [9] S. Hecker, M. Blothe, D. Grossmann, and T. Graf: *Appl. Opt.*, 59, (2020) 6452.
- [10] S. Hecker, M. Scharun, and T. Graf: *Appl. Opt.*, 60, (2021) 3526.

(Received: June 16, 2023, Accepted: September 15, 2024)